doi:10.2533/chimia.2007.826 CHIMIA **2007**, *61*, No. 12

Chimia 61 (2007) 826–830

ISSN 0009–4293

Ultrahigh Vacuum Preparation and Passivation of Abrupt SiO_2/Si(111) Interfaces

Bert Stegemann*[a], Daniel Sixtensson[a], Thomas Lussky[a], Ulrike Bloeck[b], and Manfred Schmidt[a]

Abstract: Compositionally and structurally abrupt Si/SiO_2 interfaces were prepared under ultrahigh vacuum conditions by RF plasma oxidation of Si(111) substrates with thermalized neutral oxygen atoms. The chemical, structural and electronic properties of the interface were analyzed and discussed with respect to a possible application in photovoltaic Si/SiO_2 quantum well structures. The benefits of using neutral atomic oxygen were explored and turned out to be manifold: ultrathin SiO_2 layers (thickness: 1–2 nm) can be precisely grown, the formation of suboxides is mostly suppressed and abrupt Si/SiO_2 interfaces are obtained even at moderate substrate temperatures of 300 to 600 °C. Due to the perfect Si/SiO_2 interfaces, the SiO_2 layers allow thermal post-oxidation treatment up to 1000 °C without significant change in oxide thickness or stoichiometry. This is an essential prerequisite for the envisaged realization of Si/SiO_2 superlattices with high crystallinity and low strain. It was shown that a post-oxidation annealing step lowers the strain and disorder at the interface resulting in lower intrinsic density of interface states. A further decrease of the density of interface states was achieved by hydrogen passivation as a result of saturation of dangling bonds.

Keywords: Atomic oxygen · Density of interface states · Hydrogen · Nanostructures · X-ray photoelectron spectroscopy

Introduction

The thermodynamic efficiency for solar energy conversion into electrical energy is generally limited by the bandgap energy of the absorber material. Assuming detailed balance and a single junction silicon absorber (bandgap energy 1.12 eV) the maximum conversion efficiency was determined by Shockley-Queisser to be 32.7%.[1] The main factor responsible for losses is the mismatch of solar spectrum and absorber bandgap energy. Photons with energies below the bandgap are not absorbed and whereas photons with energies above the bandgap generate hot charge carriers which lose their excess energy during thermalization to their respective band edges.

In recent years, several concepts to enhance photovoltaic efficiencies by circumventing the Shockley-Queisser limit, often termed as third generation photovoltaics, have been proposed.[2] A promising approach to enhance conversion efficiencies by overcoming losses of excess energy of photogenerated carriers is to realize stacked or tandem structures consisting of absorbers with different bandgap energies adapted to the solar spectrum. For multiple bandgap III-V compound triple junction solar cells efficiencies of up to 40% have been successfully demonstrated recently.[3] With respect to its dominant position in photovoltaics silicon attracts particular attention and is currently under active investigation in order to engineer wide bandgap absorbers by utilizing quantum size effects in silicon-based nanostructures.[4–7] Bandgap tuning can be achieved when the dimensions are reduced down to a size range where quantum effects appear and the bandgap energy becomes size-dependent. This can be realized in nanoscale silicon/silicon dioxide (Si/SiO_2) heterostructures, such as multiple quantum wells (QWs) with well thicknesses of less than about 10 nm. Further, when the SiO_2 barrier is sufficiently thin (<4 nm) superlattices (SLs) are obtained which form minibands due to strong electronic coupling between the wells allowing for efficient carrier transport.[8–10] Due to the large band offset at the Si/SiO_2 interface ($\Delta E_V \approx 4.5$eV[11]) the QWs formed are much deeper than those in III-V heterostructures, which provides more accessible quantum states and utilizes quantum phenomena even at room temperature.[12]

However, several fundamental issues need careful attention before photovoltaic devices based on Si/SiO_2 multiple QWs or SLs can become prevalent in applications. As solar cell performance is generally limited by the active optical volume, a large number of stacked Si QWs is essential to achieve sufficient light absorption. But, as the increase of the number of QWs is inherent with an increasing number of interfaces, charge carrier recombination and scattering is facilitated. These effects result in a lower mobility lifetime product ($\mu\cdot\tau$) and, thus, a lower efficiency. To overcome this drawback, for the realization of Si/SiO_2 SLs experimental methods are required that are capable of preparing pure, uniform and ultrathin Si and SiO_2 layers with abrupt Si/SiO_2 interfaces, which should have low densities of defect states. The basic component of any Si/SiO_2 SL is the Si/SiO_2 interface. Accordingly, the present study focuses on well-defined preparation of ultrathin SiO_2

*Correspondence: Dr. B. Stegemann[a]
Tel.: +49 30 8062 1313
Fax: +49 30 8062 1333
E-Mail: bert.stegemann@hmi.de
[a]Hahn Meitner Institute Berlin GmbH
Department of Silicon Photovoltaics
Kekuléstr. 5
D-12489 Berlin, Germany
[b]Hahn Meitner Institute Berlin GmbH
Department of Dynamics of Interfacial Reactions
Glienicker Str. 100
D-14109 Berlin, Germany

layers on single crystalline Si substrates under ultrahigh vacuum conditions and the careful *in situ* interface analysis of its structural, compositional and electronic properties with respect to the proposed preparation of photovoltaic Si/SiO_2 nanostructures.

Experimental

Si/SiO_2 interface were prepared by oxidation of 2" Si(111) float zone wafers (1–2 Ωcm) under ultrahigh vacuum (UHV) conditions (base pressure of $<3 \times 10^{-9}$ mbar). Prior to transfer into the UHV chamber, native oxide was removed from the Si wafer by the RCA procedure followed by etching in 1% aqueous hydrofluoric (HF) acid for 60 s, rinsing in deionized water and drying under flowing nitrogen. This procedure produces a Si(111):H-1×1 surface with a microroughness of 0.6 nm that prevents oxide formation for a few minutes.[13] In UHV clean and atomically flat surfaces were produced by heating the sample radiatively to 1000 °C. Successful cleaning was confirmed by monitoring the characteristic 7×7 reconstruction pattern of Si(111) by RHEED (reflection high energy electron diffraction). Ultrathin SiO_2 layers were prepared by oxidation of the heated Si substrate with neutral atomic oxygen using a radio frequency (RF) plasma cracker source (PCS-RF, Oxford Scientific). A special aperture with an ion trap allows just neutral atoms to effuse out of the source. These oxygen atoms are mainly thermalized (E_{kin} <1 eV) when impinging the substrate surface. The pressure during oxidation was kept at 2×10^{-6} mbar, oxidation time was typically 15 min and RF plasma powers of P_{RF} = 300–400 W were applied.

After preparation, the samples were transferred to the analysis chamber ($<1 \times 10^{-10}$ mbar) without breaking the vacuum for analysis by X-ray photoelectron spectroscopy (XPS) with non-monochromatic Mg Kα X-ray excitation (1253.6 eV) and a hemispherical energy analyzer (Specs EA10P) at a pass energy of 30 eV. For further analysis the samples were transferred to air.

To investigate the influence of interface passivation with hydrogen, some samples were annealed at 420 °C for 20 min in forming gas (*i.e.* 10% H_2 in N_2) within a quartz-tube furnace. For surface photovoltage (SPV) measurements the sample under test became part of an artificial metal-insulator-semiconductor structure (MIS), *i.e.* it was sandwiched between a sheet of mica with a transparent conductive front contact and a metallic back contact, as described in detail elsewhere.[14] Upon illumination of the sample *via* the front contact with an intense laser pulse (1.36 eV, 162 ns) excess charge carriers were created leading to band flattening and quasi Fermi level split up. These charge redistribution was measured capacitively as photovoltage. The energetic distribution of the density of states $D_{it}(E)$ at the Si/SiO_2 interface was determined from the dependence of the photovoltage on an external field applied perpendicular to the sample.[15]

Results and Discussion

XPS is a well-established technique for determination of the surface composition (stoichiometry and chemical states of the different elements) as well as for quantitative estimation of the thickness of an overlayer. Fig. 1 shows the Si 2p spectra of a Si(111) wafer after RF plasma oxidation (P_{RF} = 400 W, t = 30 min) with neutral atomic oxygen at substrate temperatures varying from room temperature (RT) up to T_{sub} = 1000 °C. Generally, Si 2p spectra of such structures are interpreted in terms of five oxidation states Si^{n+} (n = 0–4), which have identical line shapes except that the Gaussian width increases progressively for higher oxidation numbers due to increased local disorder when going from crystalline Si to amorphous SiO_2. During oxidation, homopolar Si–Si bonds are step-by-step replaced by heteropolar Si–O bonds. The charge transfer from Si to the more electronegative O leaves a positive charge on Si, which results in a shift of the Si core-levels towards higher binding energies E_B by ~1 eV for each Si–Si bond that is replaced by a Si–O bond. The thickness of the oxide t_{ox} layer can be estimated from the relative peak areas. For this, a constant inelastic mean free path of 3 nm was assumed.[16,17]

The curves in Fig. 1 generally exhibit a variably pronounced double peak structure with a peak separation of about 4 eV, which can identified as oxidation states Si^{0+} and Si^{4+}, corresponding to Si and SiO_2, respectively. All curves are normalized to the intensity of the Si^{0+} signal. It is seen that the Si^{4+} signal, and thus the oxide thickness, is maximal at T_{sub} = 300 and 600 °C, whereas the Si^{4+} signal decreases when approaching T_{sub} = RT or 1000 °C. These findings indicate that UHV oxidation with atomic oxygen does not require high temperatures. Even at room temperature the growth of a thin oxide layer ($t_{ox} \approx 0.7$ nm) is enabled,

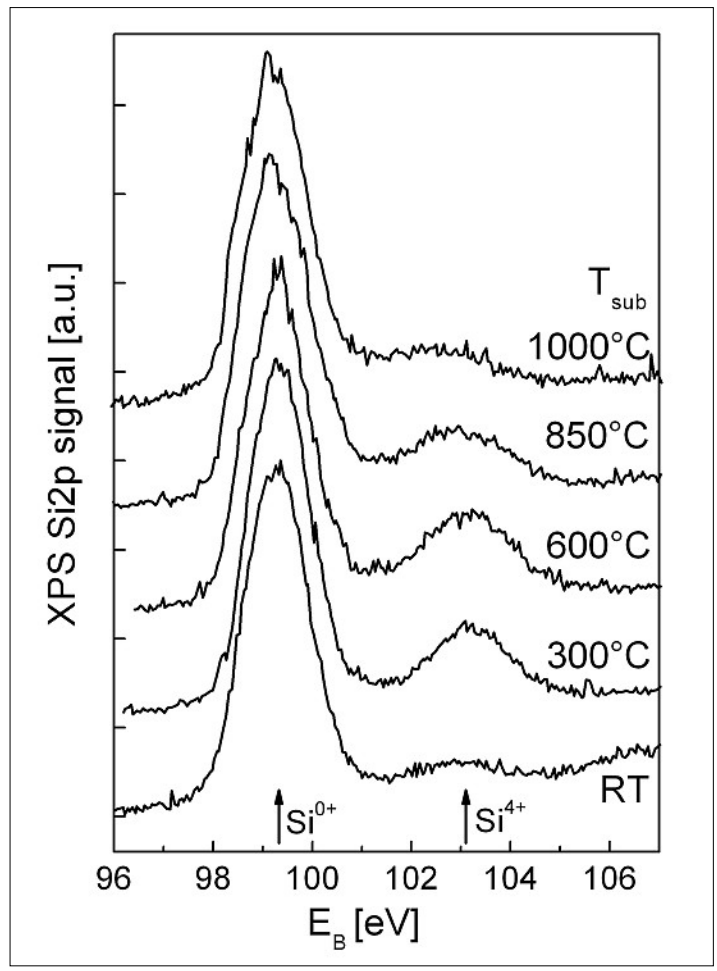

Fig. 1. Si 2p XPS spectra of the Si(111) wafer after RF plasma oxidation with thermalized neutral oxygen atoms at different substrate temperatures ranging from room temperature (RT) to 1000 °C. Oxidation parameters: P_{RF} = 300–400 W, t = 15 min.

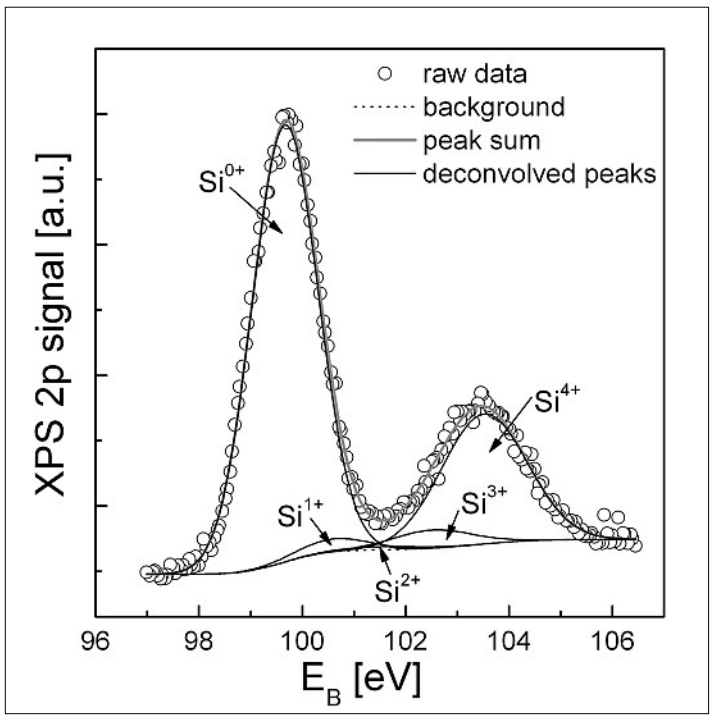

Fig. 2. Line shape analysis with a Shirley background elucidating contributions mainly from the oxidation states Si^{0+} and Si^{4+}, corresponding to Si and SiO_2, respectively. Minor amounts of Si^{1+}, Si^{2+} and Si^{3+} are revealed. Relative peak areas: Si^{0+}: 67.8%, Si^{1+}: 2.1%, Si^{2+}: 0.6%, Si^{3+}: 3.3%, Si^{4+}: 26.2%.

but oxide thickness saturates early due to the slower oxidation rate at low temperatures.[18] Most efficient SiO_2 layer growth was found to occur at moderate substrate temperatures between T_{sub} = 300 and 600 °C ($t_{ox} \approx 2$ nm), whereas at higher temperatures the rise of the desorption rate becomes effective resulting in decreased oxide thickness. T_{sub} was found to be the main parameter affecting the oxide thickness at given plasma power, because after a very fast initial oxidation step completed within a few minutes, oxidation almost saturates regardless of the oxidation time. However SiO_2 thickness control is still possible in the range from 1 to 4 nm by appropriate adjustment of the plasma power, as we reported earlier.[7] For the following investigations oxide layers were prepared at the upper limit of the process window (*i.e.* T_{sub} = 600 °C), because higher temperatures are considered to decrease interface roughness and interface trap densities.[19]

Peak analysis by appropriate Gaussian curve fitting after Shirley background subtraction is demonstrated in Fig. 2 for the case of an XPS Si 2p spectrum of oxide layer obtained at T_{sub} = 600 °C. The deconvolution confirms the principal assignment of the two peaks to Si^{0+} and Si^{4+}. Just minor amounts of the intermediate oxidation states Si^{1+}, Si^{2+} and Si^{3+} were detected, mainly represented by Si^{1+} and Si^{3+}. This is in qualitative accordance with the results from Hirose *et al.,* who found that the total density of the intermediate oxidation states is constant at an abrupt interface and mainly made up of Si^{1+} and Si^{3+} atoms.[20] The thickness of the SiO_2 layer as estimated from the relative peak areas is about 2 nm. Thus, we can conclude that by UHV plasma oxidation with thermalized, neutral atomic oxygen a pure SiO_2 layer is formed on top of the Si layer with a nearly abrupt interface. The abrupt interface points towards a progressively decreasing activation energy for each successive substitution of a Si–Si bond by a Si–O bond, *i.e.* subsequent oxidation of an intermediate Si oxidation state is energetically more favorable than initial oxidation of a Si^{0+} atom.

Hyperthermal (5 eV) atomic oxygen[21] as well as atomic oxygen dissociated from ozone[22] were also found to suppress the formation of suboxides at the SiO_2/Si interface, leading to a stable Si–O–Si network formation even at low pressure and low temperature. In addition, the existence of no (or a very thin) structural transition layer was suggested from these results, while those experiments for thermally grown oxide showed the existence of a transition layers with a thickness of approximately 1 nm.[22] Moreover, oxidation with molecular oxygen is less efficient, since it is known that it has a lower adsorption probability[23] and a higher activation energy for diffusion both in Si and SiO_2.[24] Oxidation with exclusively neutral atoms might also have a favorable effect for the structure of the oxide and the Si/SiO_2 interface.[24] However, further understanding is necessary to take control of the different roles of neutral and charged oxidizing species and the resulting opportunities for further optimization of the interface properties.

High resolution transmission electron microscopy (TEM) was applied to provide information on homogeneity and thickness of the SiO_2 layer in direct space. As seen in the cross sectional image in Fig. 3, the SiO_2 layer appears amorphous and possesses a uniform thickness of about 2 nm. There are no indications for voids or cavities. The interface appears structurally flat without any apparent interfacial layer. The surface roughness, as measured by atomic force microscopy, was typically 0.1 nm. Thus, two-dimensional oxide growth is confirmed, and it can be concluded that the interface is not only chemically but also structurally abrupt.

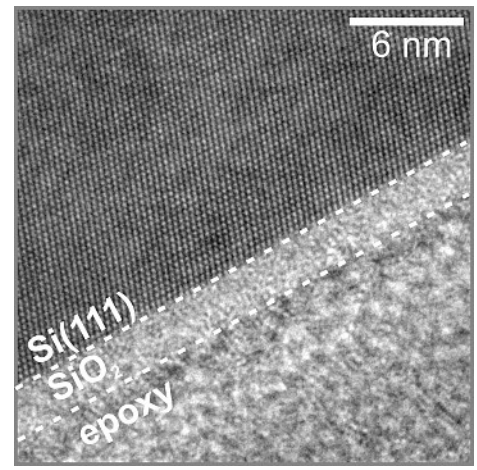

Fig. 3. High-resolution TEM image of the cross-section of the ultrathin SiO_2 layer on Si(111) with a uniform thickness of 2 nm

In the following the effect of post-oxidation annealing at 1000 °C on the oxide properties is discussed. For this purpose the XPS signal of the Si 2p transition was recorded before and after vacuum annealing the sample at 1000 °C as shown in Fig. 4a. Apparently, there is no change, meaning that neither stoichiometry nor thickness of the oxide is affected upon thermal annealing in UHV environment. This behavior is in contrast to the removal of, *e.g.* thermal oxide by annealing at 875 °C. Thermal oxide removal was found to be mediated by SiO_x complexes that react with mobile Si monomers at the silicon/oxide interface. By this reaction SiO is formed which desorbs from the surface. The high thermal stability of the SiO_2 layer prepared by UHV plasma oxidation with neutral atomic oxygen is considered to be a strong indicator for the absence of suboxides as well as the high structural quality of the interface. This result is also of importance for the envisaged preparation of Si/SiO_2 SLs, since it

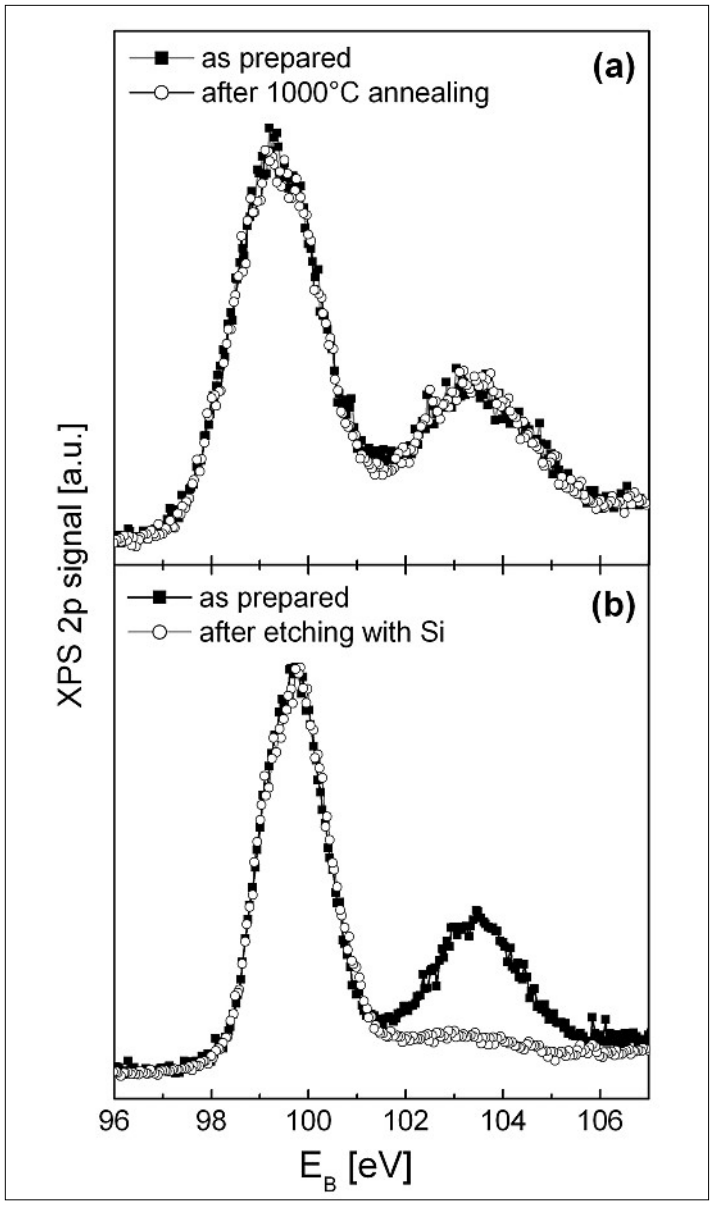

Fig. 4. Si 2p XPS spectra of the oxidized Si(111) wafer (a) before and after UHV annealing for 10 min at T_{sub} = 1000 °C, (b) before and after thermal deposition of 1 nm Si at T_{sub} = 850 °C at 0.1Å/s .

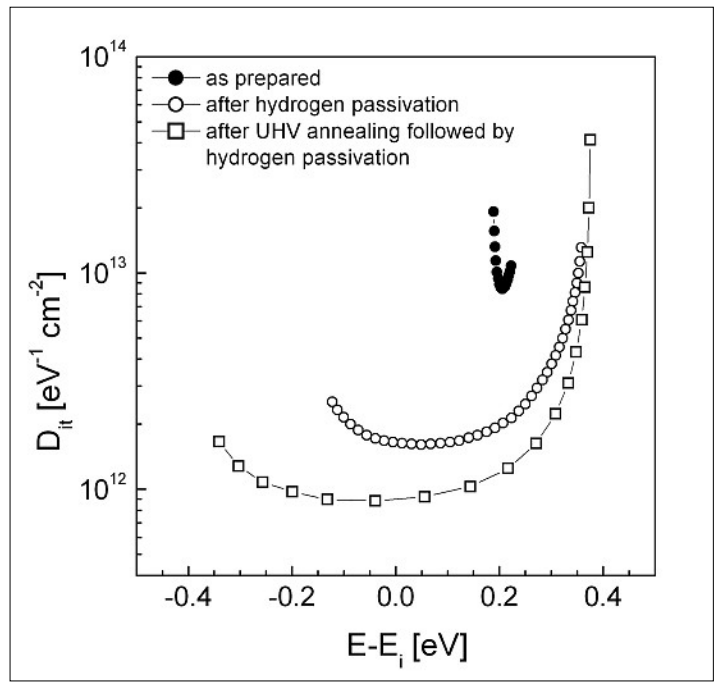

Fig. 5. Distribution of the density of states at the SiO_2/Si(111) interface D_{it} relative to the Fermi level E_i of intrinsic Si as determined from field-dependent SPV measurements ($t_{ox} \approx 2$ nm).

allows the crystallization of the Si layers that are sandwiched by SiO_2 and initially in the amorphous state while maintaining the overall sample configuration. As shown previously, crystallization of 10 nm a-Si QWs requires temperatures as high as 1000 °C.[7] This temperature is higher than the common crystallization temperature of bulk a-Si of about 700 °C due to increased interface binding energies at decreasing layer thickness.[25]

Though being stable against thermal treatment, it is possible to remove the SiO_2 layer by exposing the sample to a low silicon flux from an electron beam evaporator if the substrate is held at the typical onset temperature of oxide desorption. Fig. 4b shows the XPS Si 2p signal after preparation of a 2 nm thick SiO_2 layer and after etching off the oxide at an extremely low oxygen flux (0.1 Å/s, total nominal deposited amount: 1nm) and T_{sub} = 850 °C. The impact of Si leads to a reduction of SiO_2, supposedly initiated at the dangling bonds of the terminating Si and O atoms at the amorphous SiO_2 surface.[26,27] This scenario is principally similar to the oxide reduction at the silicon/silicon oxide interface during thermal oxide removal as described before. Supplying the proper amount of Si would also allow a controlled thinning of the SiO_2 layers and, thus, a more accurate adjustment of the SiO_2 barrier thickness in the SLs.

The influence of hydrogen passivation in forming gas and of a post-oxidation UHV annealing step on the SiO_2/Si(111) interface state density as determined from field-dependent SPV measurements is revealed in Fig. 5. There is a clear qualitative change of the measured distribution of gap states before and after hydrogen passivation. The density of gap states decreases by roughly one order of magnitude and the width of the measured distribution increases significantly. The former is considered to result from saturation of dangling bonds and thereby elimination of defect states by hydrogen, while the latter is due to removal of the Fermi-level pinning in the passivated sample. Fermi-level pinning is due to high defect densities in the band gap which impedes field induced band bending. SPV measurements suffer from the prerequisite that the band bending must be swept over the whole energy range where one wishes to measure the interface density of gap states.[28] Therefore, in cases of high defect densities at the interface the measurable region becomes very narrow. The effect of hydrogen passivation can clearly be attributed to passivation of defects located in the band gap. After hydrogen passivation, remaining to be seen is the intrinsic U-shaped distribution of interface gap states. This distribution is a consequence of the lattice mismatch between Si/SiO_2 resulting in strain and disorder near the interface.[14,29,30] Notable is that a post-oxidation annealing step seems to lower the strain and disorder at the interface resulting in lower intrinsic density of interface states as can be seen in Fig. 5.

Conclusions

Bandgap control of silicon-based material provides a promising way towards next generation photovoltaic devices such as tandem solar cells. Such bandgap control can be achieved by silicon nanostructures

consisting of Si/SiO_2 QWs or SLs. The basic component of all of these structures is the Si/SiO_2 interface. The present study explored the well-defined preparation of ultrathin SiO_2 layers on single crystalline Si substrates under UHV conditions and the careful *in situ* analysis of the interface properties.

UHV oxidation of Si(111) wafers with thermalized neutral oxygen atoms at moderate substrate temperatures of 300 to 600 °C was proven to produce ultrathin, uniform SiO_2 layers with compositionally and structurally abrupt Si/SiO_2 interfaces. Due to the perfect Si/SiO_2 interfaces, the SiO_2 layers allow thermal post-oxidation treatment up to 1000 °C without significant change in oxide thickness or stoichiometry. This is an essential prerequisite for the envisaged realization of photovoltaic Si/SiO_2 superlattices with high crystallinity and low strain. It was shown that a post-oxidation annealing step lowers the strain and disorder at the interface resulting in lower intrinsic density of interface states D_{it} and thus enhances the interface properties. A further decrease of D_{it} was achieved by hydrogen passivation as a result of saturation of dangling bonds.

With respect to application in photovoltaics this study needs to be extended to Si/SiO_2 single and multi QW structures. For these structures it is imperative not only to prepare high quality interfaces but also highly crystalline Si layers with preferred crystallographic orientation to avoid additional losses due to gain boundary induced defects.

Acknowledgments

The authors are grateful to A. Schoepke for fruitful discussions, and to D. Patzek, M. Schulz and K. Jacob for experimental and technical support. This work is funded by the Bundesministerium für Bildung und Forschung (BMBF joint project 03SF0308).

Received: October 15, 2007

[1] W. Shockley, H. J. Queisser, *J. Appl. Phys*. **1961**, *32*, 510.
[2] M. A. Green, 'Third Generation Photovoltaics. Advanced Solar Energy Conversion', 2nd ed., Springer, Berlin, **2005**.
[3] R. R. King, D. C. Law, K. M. Edmondson, C. M. Fetzer, G. S. Kinsey, H. Yoon, R. A. Sherif, N. H. Karam, *Appl. Phys. Lett*. **2007**, *90*, 183516.
[4] G. Conibeer et al., *Thin Solid Films* **2006**, *511*, 654.
[5] C. W. Jiang, M. A. Green, *J. Appl. Phys*. **2006**, *99*, 114902.
[6] R. Rolver, M. Forst, O. Winkler, B. Spangenberg, H. Kurz, *J. Vac. Sci. Techn*. **2006**, *A 24*, 141.
[7] B. Stegemann, A. Schoepke, M. Schmidt, *J. Non-Cryst. Sol*. **2007**, in press.
[8] N. Tit, M. W. C. Dharma-Wardana, *J. Appl. Phys*. **1999**, *86*, 387.
[9] T. Takagahara, K. Takeda, *Phys. Rev*. **1992**, *B 46*, 15578.
[10] T. Zheng, Z. Li, *Superlattices and Microstructures* **2005**, *37*, 227.
[11] F. J. Grunthaner, P. J. Grunthaner, *Mat. Sci. Rep*. **1986**, *1*, 65.
[12] D. J. Lockwood, Z. H. Lu, J. M. Baribeau, *Phys. Rev. Lett*. **1996**, *76*, 539.
[13] H. Angermann, W. Henrion, M. Rebien, D. Fischer, J.-T. Zettler, A. Röseler, *Thin Solid Films* **1998**, *313*, 552.
[14] W. Fussel, M. Schmidt, H. Angermann, G. Mende, H. Flietner, *Nucl. Instr. Meth. Phys. Res.* **1996**, *A 377*, 177.
[15] Y. W. Lam, *J. Phys*. **1971**, *D4*, 1370.
[16] F. J. Himpsel, F. R. McFeely, A. Taleb-Ibrahimi, J.A. Yarmoff, G. Hollinger, *Phys. Rev. B* **1988**, *38*, 6084.
[17] K. Joong Kim, K. T. Park, J. W. Lee, *Thin Solid Films* **2006**, *500*, 356.
[18] T. Majamaa, O. Kilpela, S. Novikov, *Appl. Surf. Sci.* **1998**, *136*, 17.
[19] H. Fukuda, M. Yasuda, T. Iwabuchi, S. Kaneko, T. Ueno, I. Ohdomari, *J. Appl. Phys.* **1992**, *72*, 1906.
[20] K. Hirose, H. Nohira, K. Azuma, T. Hattori, *Progr. Surf. Sci*. **2007**, *82*, 3.
[21] M. Kisa, T. K. Minton, J. C. Yang, *J. Appl. Phys*. **2005**, *97*, 023520.
[22] S. Ichimura, A. Kurokawa, K. Nakamura, H. Itoh, H. Nonaka, K. Koike, *Thin Solid Films* **2000**, *377*, 518.
[23] J. R. Engstrom, M. M. Nelson, T. Engel, *J. Vac. Sci. Tech*. **1989**, *A 7*, 1837.
[24] M. A. Szymanski, A. M. Stoneham, A. Shluger, *Solid-State Electr*. **2001**, *45*, 1233.
[25] M. Zacharias, P. Streitenberger, *Phys. Rev. B* **2000**, *62*, 8391.
[26] D. A. Luh, T. Miller, T. C. Chiang, *Phys. Rev. Lett*. **1997**, *79*, 3014.
[27] G. D. Wilk, Y. Wei, H. Edwards, R. M. Wallace, *Appl. Phys. Lett*. **1997**, *70*, 2288.
[28] L. Kronik, Y. Shapira, *Surf. Sci. Rep*. **1999**, *37*, 1.
[29] E. H. Poindexter, P. J. Caplan, *Prog. Surf. Sci.* **1983**, *14*, 201.
[30] J. Singh, A. Madhukar, *J. Vac. Sci. Techn.* **1981**, *19*, 437.